Acta Chemica Scandinavica A 29 (1975) 623—631

On the Crystal Structures of TiS_3, ZrS_3, $ZrSe_3$, $ZrTe_3$, HfS_3, and $HfSe_3$

SIGRID FURUSETH, LEIF BRATTÅS and ARNE KJEKSHUS

Kjemisk Institutt, Universitetet i Oslo, Blindern, Oslo 3, Norway

Structure determinations of TiS_3, ZrS_3, $ZrSe_3$, $ZrTe_3$, HfS_3, and $HfSe_3$ on the basis of three-dimensional single crystal X-ray data have revealed that the $ZrSe_3$ type structure occurs in two variants, here termed A and B. Variant A matches the earlier found $ZrSe_3$ type, whereas variant B corresponds to a kind of mirror image. Kinetic factors associated with the crystal growth are believed to be responsible for the occurrence of these two variants.

The trichalcogenides of titanium, zirconium, hafnium, thorium, and uranium are believed to be isostructural with $ZrSe_3$, whereas various assignments of this structure type to niobium and tantalum trichalcogenides have proved to be incorrect (*cf. e.g.*, Refs. 1 – 4 and references therein). Except for $ZrSe_3$, the compounds have been classified structurally on the basis of similarities in their X-ray powder patterns. Proper structure determinations of compounds which have previously been only superficially classified need not necessarily be a trivial task, and the present work on the structures of TiS_3, ZrS_3, $ZrSe_3$, $ZrTe_3$, HfS_3, and $HfSe_3$ may serve as an example of this.

EXPERIMENTAL

Single crystals of TiS_3, ZrS_3, $ZrSe_3$, $ZrTe_3$, HfS_3, $HfSe_3$, and $HfTe_3$ were prepared earlier by means of chemical transport reactions.[4] A new compound $TiSe_3$ was prepared similarly [from 99.99 % Ti (A. D. Mackay) and 99.998 % Se (Bolidens Gruvaktiebolag)], using ~350 °C for the cold point and 100 to 150 °C for the temperature difference between the hot and cold regions. Details specifying relevant characteristics for the crystals subject to this study are recorded in Table 1.

Single crystal X-ray data for each compound were collected photographically, using the Weissenberg technique and Zr-filtered Mo$K\alpha$-radiation. The $TiSe_3$ and $HfTe_3$ crystals obtained so far, have proved to be unsuitable for structure determinations. For the other compounds, three-dimensional intensity data were obtained from integrated Weissenberg films. The intensities were measured microphotometrically except for the weakest reflections, which were estimated visually.

A supplementary set of data for TiS_3 was collected with an automatic Picker diffractometer. The $\omega - 2\theta$ scan technique was utilized at a scan speed of 1° min^{-1} up to $\sin\theta/\lambda = 0.8$. The background was measured at each of the scan range limits. The intensities of three selected test reflections, measured for every 50th reflection during the data collection, demonstrated a systematic variation which was corrected for in the sets of observed intensities. A graphite crystal was used for monochromatization, the scan range was $2\theta(\alpha_1) - 0.9$ to $2\theta(\alpha_2) + 0.9°$, and the background was measured for 30 s on each side of the reflections. Reflections with $I_{net.} \leqq 1.5\sigma(I)$ were regarded as unobserved.

As is evident from Table 1, needle shaped crystals are characteristic for compounds belonging to the $ZrSe_3$ family. The monoclinic b axis is always oriented along the needle axis. The actual shapes of the crystals were evaluated with the aid of an optical goniometer in combination with a travelling microscope. Apart from two cases (see Table 1), absorption corrections were carried out in accordance with the actual crystal shapes. (No corrections for dispersion and secondary extinctions were performed.)

The computational work, including corrections, data reductions, scalings, Patterson- and Fourier-syntheses, full matrix least squares refinements of the structure factors, and calculations of interatomic distances and angles was carried out using programmes of Groth.[5]

Atomic scattering factors were taken from

Table 1. Specifications of single crystal specimens (for abreviations A, B, and Tw see text). Data were recorded on Weissenberg films.

Compound [a]	No. of crystals tested	Crystal type (% occurrence)	Crystal dimensions (mm)	Crystal shape for absorption correction	Total No. of reflections (unobserved)	No. of reflections for least squares refinement
TiS_3	8	B(~90 %),Tw(~10 %)	0.010×0.030×0.95 0.015×0.040×0.80 [b]	Cylindrical As observed [b]	382(139) 654(327) [b]	243 316 [b]
ZrS_3	12	A(~85 %),Tw(~15 %)	0.012×0.033×1.87	As observed	604(250)	353
$ZrSe_3$	13	A(~90 %),Tw(~10 %)	See Ref. 1			
$ZrTe_3$	10	B(~90 %),Tw(~10 %)	0.020×0.020×0.305	As observed	622(290)	322
HfS_3	14	A(~90 %),Tw(~10 %)	0.009×0.025×0.294	Cylindrical	581(143)	425
$HfSe_3$	15	B(~70 %),A(~15 %), Tw(~15%)	0.008×0.032×0.312	As observed	593(192)	400

[a] $TiSe_3$ and $HfTe_3$ were unsuitable for structure determination. [b] Data recorded with diffractometer (counter).

Hanson *et al.*[6] Anisotropic thermal motion of the atoms was allowed for according to the expression $\exp[-(\beta_{11}h^2+\beta_{22}k^2+\beta_{33}l^2+\beta_{12}hk+\beta_{13}hl+\beta_{23}kl)]$. The extent of agreement between the observed and calculated structure factor data is judged from the average and weighted reliability factors $R=\sum||F_o|-|F_c||/\sum|F_o|$ and $R^*=[\sum w(|F_o|-|F_c|)^2/\sum w|F_o|^2]^{\frac{1}{2}}$ where w denotes the weight factor. (The observed and calculated structure factor data are available from the authors upon request.)

RESULTS

(i) *Homogeneity ranges and compositions.* Phase analyses by visual and microscopic inspection, X-ray diffraction, and density measurements, as well as chemical analyses of suitable single crystal specimens, have unequivocally showed (*cf.* Ref. 4) that all compounds subject to this study obtain the stoichiometric 1:3 composition without appreciable ranges of homogeneity. The question of non-stoichiometry and homogeneity ranges has been considered for the zirconium and hafnium trichalcogenides in a recent paper by Jellinek *et al.*[7]; they conclude that chalcogen-deficiency (*viz.* TX_{3-x}; where T=Ti, Zr, or Hf, X=S, Se, or Te, and $x>0$) seems likely for these compounds. The inferences of Jellinek *et al.* are apparently based on results reported in Refs. 8 and 9. McTaggart and Wadsley's [8] work cannot be taken as a support for this view, since they state that "there is little chemical evidence to suggest that the trichalcogenides are anything but stoichiometric". Schairer and Shafer,[9] on the other hand, explicitly state that ZrS_3 and HfS_3 both take "a rather large range of stoichiometry (*i.e.* metal-sulfur ratios)". Their deductions are based on quantitative analyses of single crystal specimens of the two compounds, grown under different thermal conditions (by chemical transport reactions). A large number of single crystal batches for most of the compounds subject to this study have been obtained under a variety of different thermal conditions. Careful examinations of these have invariably confirmed a stoichiometric $TX_{3.00\pm0.04}$ composition, where the error limits are imposed by the inherent uncertainties of the experimental techniques.

The unit cell dimensions of the Ti, Zr, and Hf trichalcogenides (as determined by least squares refinements of Guinier powder photographic data) are listed in Table 2. These, together with the observed densities,[4] show that the unit cell content is 2 TX_3 groups for

Table 2. Unit cell dimensions for compounds with the $ZrSe_3$ type structure (variants A and B); values are quoted from Ref. 4.

Compound	a (Å)	b (Å)	c (Å)	β (°)
TiS_3	4.958(2)	3.4006(11)	8.778(4)	97.32(4)
ZrS_3	5.1243(11)	3.6244(10)	8.980(3)	97.28(2)
$ZrSe_3$	5.4109(12)	3.7488(9)	9.444(2)	97.48(2)
$ZrTe_3$	5.8939(14)	3.9259(12)	10.100(2)	97.82(2)
HfS_3	5.0923(11)	3.5952(7)	8.967(2)	97.38(2)
$HfSe_3$	5.388(2)	3.7216(10)	9.428(3)	97.78(3)
$HfTe_3$	5.879(2)	3.9022(9)	10.056(3)	97.98(3)

all compounds.

(ii) *Structure determinations.* The only systematic extinctions in the diffraction data for all crystals subject to this study are of the type $0k0$ absent when $k=2n+1$, leaving a choice between $P2$, $P2_1$, Pm, $P2/m$, and $P2_1/m$ for the space group. In accordance with the results of Krönert and Plieth [1] for $ZrSe_3$, the correct space group proved to be $P2_1/m$.

The clear-cut relationships in composition, crystal shapes, unit cell dimensions, X-ray powder diffraction intensity data, and space group suggested very strongly that all the group IV A trichalcogenides are isostructural with $ZrSe_3$.[1] HfS_3 was more or less arbitrarily chosen as the first object for examination in this programme. The results for this compound (Table 3) indeed confirmed that it adopts the assumed $ZrSe_3$ type structure. This finding further reinforced our presentiments of a plain and unchallenging research programme merely designed to provide values for interatomic distances and angles.

Already the next member of the family studied, TiS_3, gave unexpected results, which forced us to change attitude. The first set of film data for this compound lead to a structure which, although definitely related to that of $ZrSe_3$, differs in such fundamental aspects that the designation isostructural no longer applies. As a consequence, it was considered to be worthwhile to undertake a complete re-examination (by Fourier and difference syntheses as well as numerous least squares refinements starting from different initial coordinates) of the photographic data set, and finally, to collect a set of diffractometer data for another crystal. Evaluation of these data confirmed our earlier findings.

The subsequent structure determinations of ZrS_3, $ZrTe_3$, and $HfSe_3$ showed ZrS_3 to be isostructural with $ZrSe_3$, whereas $ZrTe_3$ and the first sample crystals of $HfSe_3$ turned out to be isostructural with TiS_3. Later on, another crystal of $HfSe_3$ was found that proved to be isostructural with $ZrSe_3$.

The final positional and thermal parameters for the various compounds subject to this study are listed in Table 3. Only the parameters deduced from the diffractometer data are given for TiS_3, and only values for one of the variants of $HfSe_3$.

(iii) *Twinning.* As previously documented,[1,8,10–14] twinning is frequently encountered among these TX_3 crystals. A number of crystals of each compound were examined in order to find a rough estimate for the fraction of twins (tw, see Table 1). It should be pointed out that the actual figures are unreliable since the number of crystals tested is very small. Moreover, only crystals with apparently perfect external shape and of suitable size for single crystal X-ray work were tested. On the background of Krönert and Plieth's [1] suggestions regarding the origin of the twin formation, care was taken to avoid mechanical disturbance of the crystal specimens prior to the X-ray diffraction experiments.

In close connection with the twinning phenomenon comes the observation of two variants of the $ZrSe_3$ type structure. As is evident from Table 1, a certain set of experimental conditions for a given compound results mainly in either the $ZrSe_3$ or TiS_3 form

Table 3. Positional and thermal parameters for compounds with A and B variants of the $ZrSe_3$ type structure. Space group $P2_1/m$, all atoms in position 2(*e*).

Variant		A		B			
Compound		ZrS_3	$ZrSe_3$[a]	HfS_3	TiS_3	$ZrTe_3$	$HfSe_3$
	x	0.2837(3)	0.285	0.2839(2)	0.7152(8)	0.7069(6)	0.7145(3)
	z	0.6553(2)	0.656	0.6548(1)	0.6528(3)	0.6660(4)	0.6563(2)
	β_{11}	0.0033(5)		0.0023(3)	0.0164(18)	0.0084(10)	0.0032(4)
T	β_{22}	0.0065(4)	$B=0.45$ Å^2	0.0062(3)	0.0065(14)	0.0164(8)	0.0006(3)
	β_{33}	0.0014(2)		0.0013(1)	0.0016(4)	0.0046(4)	0.0004(1)
	β_{13}	−0.0016(4)		0.0004(2)	−0.0078(14)	−0.0051(10)	−0.0061(3)
	x	0.7631(7)	0.762	0.7611(2)	0.2392(10)	0.2391(4)	0.2370(7)
	z	0.5543(4)	0.554	0.5546(7)	0.5505(5)	0.5561(3)	0.5533(4)
	β_{11}	0.0007(9)		0.0010(15)	0.0164(24)	0.0034(6)	0.0040(8)
X_I	β_{22}	0.0026(8)		0.0027(14)	0.0084(20)	0.0003(4)	0.0022(7)
	β_{33}	0.0012(3)	$B=0.45$ Å^2	0.0003(5)	0.0022(5)	0.0004(2)	0.0015(3)
	β_{13}	0.0002(8)		−0.0019(14)	−0.0104(16)	−0.0053(5)	−0.0090(9)
	x	0.4725(8)	0.456	0.4642(13)	0.5320(11)	0.5661(4)	0.5455(8)
	z	0.1716(5)	0.174	0.1702(8)	0.1762(5)	0.1676(3)	0.1733(5)
	β_{11}	0.0052(11)		0.0015(16)	0.0238(26)	0.0002(6)	0.0080(11)
X_{II}	β_{22}	0.0061(10)		0.0101(15)	0.0142(20)	0.0059(10)	0.0122(10)
	β_{33}	0.0004(3)	$B=0.45$ Å^2	0.0034(7)	0.0019(5)	0.0026(2)	0.0022(4)
	β_{13}	0.0014(11)		−0.0018(16)	−0.0081(18)	−0.0028(6)	−0.0036(10)
	x	0.8799(7)	0.888	0.8768(13)	0.1205(11)	0.0963(5)	0.1113(7)
	z	0.1699(4)	0.169	0.1697(7)	0.1737(5)	0.1616(3)	0.1673(4)
	β_{11}	0.0013(9)		0.0009(16)	0.0239(24)	0.0075(7)	0.0070(10)
X_{III}	β_{22}	0.0002(8)		0.0051(15)	0.0120(20)	0.0107(6)	0.0050(10)
	β_{33}	0.0005(3)	$B=0.45$ Å^2	0.0016(6)	0.0016(5)	0.0022(2)	0.0019(3)
	β_{13}	−0.0007(9)		0.0013(14)	−0.0121(18)	−0.0081(7)	−0.0101(10)
R		0.076	0.11	0.066	0.070	0.057	0.073
R^*		0.101	–	0.088	0.074	0.076	0.096

[a] Quoted from Krönert and Plieth.[1]

(termed the A and B variants, respectively, in Table 1 and the discussion) admixed with twins. Once again, much significance cannot be placed on the actual percentage figure given. In fact a systematic search for both of the variants was only carried out for $HfSe_3$, and even in this case the search was terminated when the less common A form had been detected for two crystals.

DISCUSSION

For description of the $ZrSe_3$ structure, reference is made to, *e.g.*, Refs. 1, 3, and 4; presently determined interatomic distances and angles (calculated from the unit cell dimensions in Table 2, and the positional parameters in Table 3) being given in Table 4.

The two variants of the $ZrSe_3$ type structure have so far been referred to as the TiS_3 and $ZrSe_3$ types. This nomenclature may serve to distract attention from the main subject by coupling the distinction to concrete members of the $ZrSe_3$ family. The atomic arrangements for both variants are illustrated in Fig. 1, using HfS_3 and $ZrTe_3$ as examples. On comparing A and B of this diagram, it is seen (neglecting the difference in scale) that the two arrangements are a kind of mirror image of each other. Thus, we adopt an alternative designation in the remainder of this paper in which the $ZrSe_3$ and TiS_3 variants are termed A and B, respectively.

Although the A and B variants are indeed almost mirror images, Fig. 1 shows that it is not a question of identity through transforma-

tion of the coordinate system. Examination of the positional parameters in Table 3 reveals that these obey the relations

$$x_A = 1 - x_B,\ y_A = y_B, \text{ and } z_A = z_B \quad (1)$$

to a very good approximation regardless of the actual compound chosen for comparison. The relations are found to hold even better for $HfSe_3$ where both variants have been examined. The results of conversion according to eqn. 1 is to simulate the behaviour of a mirror plane of symmetry parallel to (100) at $x = \frac{1}{2}$.

It is seen that the deviation of β from 90° (actually observed 97 – 98°, *cf.* Table 2) prevents perfect right/left hand identity relations between the A and B variants. This is also brought out in Fig. 2, which shows the connection between A and B in relation to the configuration of near X neighbours around a given T. The (say) A coordination polyhedron has been translated half a unit length in the direction of the a axis. Since the line connecting X_{II} and X_{III} is to a very good approximation parallel to [100], $X_{III,A}$ will then coincide with $X_{II,B}$, and similarly $X_{II,A}$ with $X_{III,B}$ in this diagram. Such an operation does not, on the other hand,

Table 4. Interatomic distances and angles in the structures of TiS_3, ZrS_3, $ZrSe_3$, $ZrTe_3$, HfS_3, and $HfSe_3$. Data referring to variant A are printed in italics.

Interatomic distances (Å) based on data from Tables 2 and 3 (quoted from Ref. 1 for $ZrSe_3$).

Compound	TiS_3	*ZrS_3*	*$ZrSe_3$*	$ZrTe_3$	*HfS_3*	$HfSe_3$
2 $T-X_I$	2.496(4)	*2.602(3)*	*2.71$_7$*	3.030(4)	*2.588(4)*	2.752(3)
1 $T-X_I$	2.416(6)	*2.724(4)*	*2.87$_0$*	2.829(4)	*2.697(6)*	2.624(4)
1 $T-X_I$	2.855(6)	*2.707(4)*	*2.86$_8$*	3.467(4)	*2.698(6)*	3.100(4)
2 $T-X_{II}$	2.667(4)	*2.602(3)*	*2.73$_3$*	3.163(3)	*2.612(5)*	2.935(4)
2 $T-X_{III}$	2.358(4)	*2.605(3)*	*2.74$_3$*	2.771(3)	*2.590(4)*	2.586(3)
$T-X$ average	2.539	*2.631*	*2.76$_6$*	3.028	*2.622*	2.784
$T-X$ scattering	0.497	*0.122*	*0.15$_3$*	0.696	*0.110*	0.514
2 $T-X_m$	2.302(4)	*2.384(3)*	*2.47$_4$*	2.634(3)	*2.379(4)*	2.508(3)
1 $X_{II}-X_{III}$	2.038(7)	*2.090(5)*	*2.34$_4$*	2.761(3)	*2.102(8)*	2.333(5)
$T-X_I$[a]	4.171(3)	*4.534(2)*	*4.72$_1$*	4.839(2)	*4.494(3)*	4.554(2)
$X_{II}-X_{III}$[a]	2.921(7)	*3.035(5)*	*3.06$_7$*	3.134(3)	*2.991(8)*	3.057(5)
$T-T$[a]	3.631(4)	*4.189(2)*	*3.74$_9$*	4.338(5)	*4.166(1)*	3.956(2)

[a] Shortest interatomic distance neglected as bonding.

Interatomic distances (Å) based on data from Tables 2 and 3 (quoted from Ref. 1 for $ZrSe_3$), but with positional parameters transformed according to eqn. 1.

Compound	*TiS_3*	ZrS_3	$ZrSe_3$	*$ZrTe_3$*	HfS_3	*$HfSe_3$*
2 $T-X_I$	*2.454(4)*	2.646(3)	2.76$_5$	*2.965(4)*	2.631(4)	*2.701(3)*
1 $T-X_I$	*2.630(6)*	2.509(4)	2.63$_5$	*3.110(4)*	2.480(6)	*2.870(4)*
1 $T-X_I$	*2.639(6)*	2.925(4)	3.10$_6$	*3.182(4)*	2.917(6)	*2.851(4)*
2 $T-X_{II}$	*2.486(4)*	2.785(3)	2.94$_0$	*2.921(3)*	2.803(5)	*2.720(3)*
2 $T-X_{III}$	*2.488(4)*	2.473(3)	2.59$_2$	*2.963(3)*	2.459(4)	*2.745(3)*
$T-X$ average	*2.516*	2.655	2.79$_2$	*2.999*	2.648	*2.757*
$T-X$ scattering	*0.185*	0.452	0.51$_4$	*0.219*	0.458	*0.169*
2 $T-X_m$	*2.267(3)*	2.418(3)	2.51$_4$	*2.594(3)*	2.418(4)	*2.467(3)*
1 $X_{II}-X_{III}$	*2.043(7)*	2.086(5)	2.33$_2$	*2.778(3)*	2.101(8)	*2.348(5)*
$T-X_I$[a]	*4.299(3)*	4.408(2)	4.58$_2$	*5.008(2)*	4.368(3)	*4.700(2)*
$X_{II}-X_{III}$[a]	*2.915(7)*	3.039(5)	3.08$_0$	*3.117(3)*	2.992(8)	*3.041(5)*
$T-T$[a]	*4.012(4)*	3.796(2)	3.97$_8$	*4.824(5)*	3.770(1)	*4.397(2)*

[a] Shortest interatomic distance neglected as bonding.

Table 4. Continued.

Interatomic angles (°) based on data from Tables 2 and 3 (quoted from Ref. 1 for $ZrSe_3$).

Compound		TiS_3	*ZrS_3*	*$ZrSe_3$*	$ZrTe_3$	*HfS_3*	$HfSe_3$
1	$T-X_I-T$	85.88(15)	*88.29(12)*	*87.3*	80.76(10)	*87.98(17)*	85.07(11)
2	$T-X_I-T$	113.20(15)	*103.83(10)*	*103.9*	115.33(9)	*103.49(16)*	113.79(10)
2	$T-X_I-T$	95.31(16)	*103.68(10)*	*104.0*	95.48(10)	*104.01(16)*	94.71(10)
1	$T-X_I-T$	140.19(20)	*141.30(15)*	*141.1*	138.63(15)	*141.42(22)*	140.41(15)
1	$T-X_{II}-T$	79.20(14)	*88.30(13)*	*86.9*	76.73(8)	*86.98(20)*	78.69(11)
2	$X_{III}-X_{II}-T$	58.32(15)	*66.41(11)*	*64.9*	55.29(8)	*65.63(18)*	57.44(10)
1	$T-X_{III}-T$	92.31(17)	*88.17(11)*	*86.2*	90.19(12)	*87.90(19)*	92.04(12)
2	$X_{II}-X_{III}-T$	74.33(18)	*66.26(11)*	*64.4*	69.73(9)	*66.72(19)*	73.07(12)
1	$T-X_m-T$	95.24(18)	*98.94(13)*	*98.5*	96.38(14)	*98.14(23)*	95.79(13)
2	$X_{II}-X_m-T$	99.56(18)	*89.91(15)*	*89.7*	99.19(14)	*90.65(20)*	99.49(12)
2	$X_{III}-X_m-T$	80.45(18)	*90.09(15)*	*90.3*	80.82(14)	*89.35(20)*	80.51(12)
1	X_I-T-X_I	85.88(13)	*88.29(10)*	*87.3*	80.76(11)	*87.98(12)*	85.07(9)
1	X_I-T-X_I	140.19(17)	*141.30(13)*	*141.1*	138.63(16)	*141.42(16)*	140.41(13)
2	X_I-T-X_{II}	93.33(10)	*86.58(9)*	*87.0*	95.95(6)	*87.06(15)*	93.62(8)
2	X_I-T-X_{III}	85.14(12)	*86.80(8)*	*87.8*	85.94(7)	*87.33(14)*	85.05(9)
1	$X_{II}-T-X_{II}$	79.20(12)	*88.30(10)*	*86.6*	76.73(9)	*86.98(15)*	78.69(8)
2	$X_{II}-T-X_{III}$	47.35(15)	*47.33(10)*	*50.7*	54.99(8)	*47.66(17)*	49.49(10)
1	$X_{III}-T-X_{III}$	92.31(15)	*88.17(9)*	*86.2*	90.19(13)	*87.90(14)*	92.04(10)
1	X_m-T-X_m	95.24(18)	*98.94(14)*	*98.5*	96.38(13)	*98.14(23)*	95.79(13)

Interatomic angles (°) based on data from Tables 2 and 3 (quotes from Ref. 1 for $ZrSe_3$), but with positional parameters transformed according to eqn. 1.

Compound		*TiS_3*	ZrS_3	$ZrSe_3$	*$ZrTe_3$*	HfS_3	*$HfSe_3$*
1	$T-X_I-T$	*87.70(15)*	86.47(11)	85.4	*82.91(11)*	86.21(16)	*87.09(12)*
2	$T-X_I-T$	*104.06(16)*	112.90(10)	113.3	*105.26(9)*	112.74(15)	*104.03(10)*
2	$T-X_I-T$	*104.17(16)*	94.84(10)	94.9	*105.13(9)*	95.02(16)	*104.19(10)*
1	$T-X_I-T$	*140.48(20)*	141.07(15)	140.8	*139.06(14)*	141.16(22)	*140.69(15)*
1	$T-X_{II}-T$	*86.33(16)*	81.21(11)	79.2	*84.45(10)*	79.78(17)	*86.35(13)*
2	$X_{III}-X_{II}-T$	*65.81(16)*	58.98(11)	57.5	*62.60(8)*	58.10(17)	*65.10(11)*
1	$T-X_{III}-T$	*86.22(16)*	94.23(13)	92.6	*82.98(10)*	93.95(21)	*85.38(11)*
2	$X_{II}-X_{III}-T$	*65.68(16)*	74.75(12)	73.1	*61.06(8)*	75.41(20)	*64.01(11)*
1	$T-X_m-T$	*97.17(18)*	97.08(13)	96.4	*98.38(14)*	96.03(22)	*97.92(13)*
2	$X_{II}-X_m-T$	*89.92(18)*	99.33(12)	99.4	*89.01(14)*	100.26(20)	*89.33(12)*
2	$X_{III}-X_m-T$	*90.08(18)*	80.67(12)	80.6	*90.99(14)*	79.74(20)	*90.67(12)*
1	X_I-T-X_I	*87.70(13)*	86.47(9)	85.4	*82.91(12)*	86.21(12)	*87.09(10)*
1	X_I-T-X_I	*140.48(17)*	141.07(13)	140.8	*139.07(16)*	141.16(17)	*140.69(13)*
2	X_I-T-X_{II}	*87.58(11)*	92.23(8)	93.1	*89.11(7)*	92.84(13)	*87.24(10)*
2	X_I-T-X_{III}	*87.97(11)*	84.01(9)	84.7	*89.75(7)*	84.54(14)	*88.23(8)*
1	$X_{II}-T-X_{II}$	*86.33(14)*	81.21(9)	79.2	*84.45(11)*	79.78(12)	*86.35(10)*
2	$X_{II}-T-X_{III}$	*48.51(15)*	46.28(10)	49.4	*56.34(8)*	46.49(17)	*50.89(10)*
1	$X_{III}-T-X_{III}$	*86.22(14)*	94.23(10)	92.6	*82.98(11)*	93.95(15)	*85.38(9)*
1	X_m-T-X_m	*97.17(18)*	97.08(13)	96.4	*98.38(14)*	96.03(22)	*97.92(13)*

bring T_A and T_B or $X_{I,A}$ and $X_{I,B}$ to even partial coincidence.

Fig. 2 also serves to illustrate that variant B has a considerably higher irregularity in the coordination polyhedron than the A variant. Consultation of Table 4 shows that the distinction between the two variants in this respect concerns mainly the scattering of the interatomic $T-X$ distances, whereas the average $T-X$ distances hardly are affected on turning

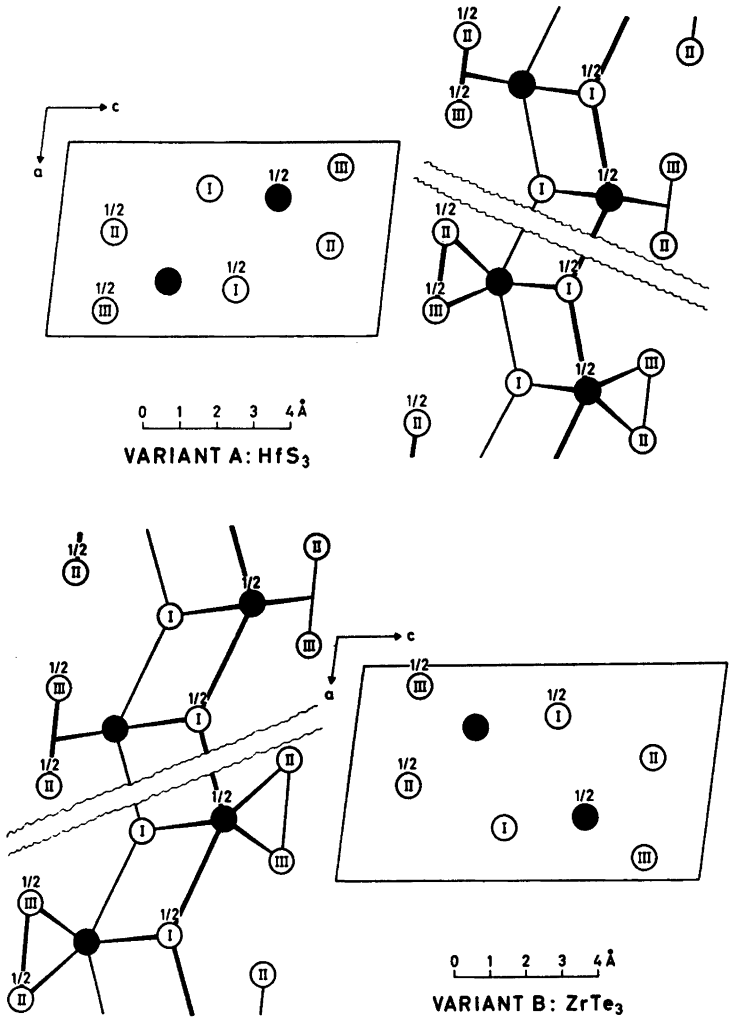

Fig. 1. Variants A and B of the $ZrSe_3$ type structure shown in (010) projection, illustrated by data obtained for HfS_3 and $HfTe_3$, respectively. Numbers give fractions of projection axis, origin being shifted to $0,\frac{1}{4},0$. Filled and open circles represent metal (T) and non-metal (X) atoms, respectively. Possible bonding paths between atoms or pairs of atoms are indicated on the right and left hand sides of the diagrams.

from the one variant to the other. As seen from Fig. 2, the irregularity of the B variant is directly related to the fact that the quasi mirror-plane relating A and B in the superimposed model intersects the line connecting X_{II} and X_{III} at an oblique angle. In the A variant, T and X_I lie approximately in the plane perpendicular to the $X_{II}-X_{III}$ pair through its mid-point X_m. Since the said perpendicular plane and the quasi mirror-plane do not coincide, this can no longer hold for the B coordination polyhedron. It should be emphasized that this merely serves to rationalize the relations between the A and B coordination polyhedra, but does not provide an explanation of the higher irregularity of the latter.

The "symmetry" relations between the A and B variants also lead to a working hypothesis for the mechanism governing the occurrence of two so closely related modifications. Since the

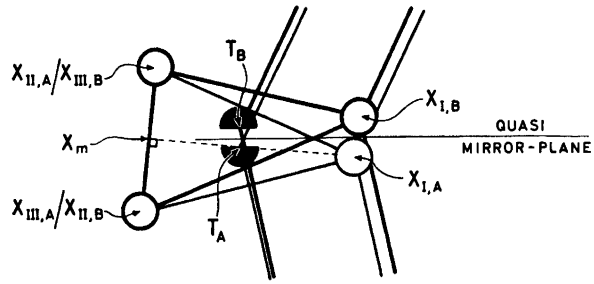

Fig. 2. Configurations of near X neighbours around T in variant A and B; superimposed to emphasize the quasi mirror-plane relationship between them.

crystals of the $ZrSe_3$ family are grown from the vapour phase (see Experimental) where kinetic factors are known to play an important role, it is natural to couple the formation of the A and B modifications to kinetics. The free energy of the two variants must be rather similar (but by no means equal) as evinced by the practically identical average values for the bonding interatomic distances (Table 4) in each case. Growth spirals (believed to be among the key factors in crystal growth) can be either right or left handed. It seems natural to associate one of the variants with a right handed growth spiral and the other with a left handed. In order to explain why this process does not lead to a corresponding rearrangement of the unit cell in relation to the coordination polyhedron, the initial crystal nuclei ought to be replicas. However, soon after nucleation the growth step occurs which initiates and determines the A/B individuality of the crystal. Experimental data over and above those available at present appear to be needed in order to resolve this problem. The future considerations should also aim at incorporating into the same model the apparently related occurrence of twinning.

All attempts [1,3,4,7] to describe the bonding situation in compounds of the $ZrSe_3$ family start with the configuration of eight near X atoms around each T. In Refs. 3 and 4 the generalized (8−N) rule is utilized to give an overall picture. Although details concerning the actual bonds do not enter into these considerations, each of the eight X atoms is apprehended as ligands bonded directly to the central T atom in a configuration described as a distorted bicapped trigonal prism. The arrangement of the bonds according to this approach is illustrated in the bottom right and left parts of Fig. 1, and the nature of all bonds is tentatively assumed to be of σ character. Jellinek *et al.*[7] have recently proposed an alternative model for the bonding in these compounds according to which each of the $X_{II}-X_{III}$ pairs is regarded as bonded to T as a single ligand. As depicted in the upper right and left parts of Fig. 1 the resulting coordination polyhedra around the central T atoms could then be described as distorted octahedra. Molecular orbitals of π symmetry on the $X_{II}-X_{III}$ fragments must in this case be considered as being used in bonding to d_π orbitals on T.

In the most extreme versions, the two models are clearly incompatible, and it is therefore appropriate at this stage to discuss their individual *pro et contra*:

(1) The assumption [1,3,4] of essentially σ bonds for $T-X_{II}$, $T-X_{III}$, and $X_{II}-X_{III}$ leads to a concentration of the valence electrons in a very restricted area of space, as evident from Fig. 1 and from the narrow interatomic angles ($X_{II}-T-X_{III}$, $T-X_{II}-X_{III}$, and $T-X_{III}-X_{II}$) listed in Table 4. This apparent disadvantage of the model in Refs. 1, 3, and 4 is clearly corrected for in the Jellinek *et al.* $X_{II}-X_{III}$ pair bonded model.

(2) Crystals with the (most symmetric) A variant of the $ZrSe_3$ type structure do not show any consistent and clear-cut distinction between the bonding interatomic distances $T-X_I$, $T-X_{II}$, and $T-X_{III}$ (Table 4). With a distinctly different bonding situation for $T-X_I$ and $T-X_m$ the model of Jellinek *et al.* seems to offer no reliable explanation for this conformity in interatomic distances. The consistent trend in the observations for the whole series of compounds can certainly not be attributed to accidental circumstances.

(3) The fact that the $ZrSe_3$ type structure

occurs in two variants appears to be indifferent to the choice between the above bonding models.

(4) The X-ray photoelectron spectra of ZrS_3 and $ZrSe_3$ and their interpretation by Jellinek *et al.* do not provide an unambiguous criterion for a choice between the two bonding models. The reason for this conclusion stems from the fact that both of the models agree on $X_{II}-X_{III}$ pairs with internal bonding, the dispute concerns only the connection between T and the $X_{II}-X_{III}$ fragment.

To summarize the situation, we conclude that both models have attractive features. It is therefore tempting to suggest their combination to a unified model, which perhaps does not make such a clear-cut distinction between symmetry and spatial location of the valence electrons. Moreover, bonding interactions resulting from effective charges may also be of importance. As an outline for future work it may be of value to perform a comparative analysis of all structures containing internally bonded non-metal pairs. Accumulation of more experimental data for the compounds belonging to the $ZrSe_3$ family will also be of utmost importance.

REFERENCES

1. Krönert, W. and Plieth, K. *Z. Anorg. Allg. Chem. 336 (1965)* 207.
2. Selte, K., Bjerkelund, E. and Kjekshus, A. *J. Less-Common Metals 11* (1966) 14.
3. Hulliger, F. *Struct. Bonding (Berlin) 4* (1968) 83.
4. Brattås, L. and Kjekshus, A. *Acta Chem. Scand. 26* (1972) 3441.
5. Groth, P. *Acta Chem. Scand. 27* (1973) 1837.
6. Hanson, H. P., Herman, F., Lea, J. D. and Skillman, S. *Acta Crystallogr. 17* (1964) 1040.
7. Jellinek, F., Pollak, R. A. and Shafer, M. W. *Mater. Res. Bull. 9* (1974) 845.
8. McTaggart, F. K. and Wadsley, A. D. *Aust. J. Chem. 11* (1958) 445.
9. Schairer, W. and Shafer, M. W. *Phys. Status Solidi A 17* (1973) 181.
10. Hahn, H. and Harder, B. *Z. Anorg. Allg. Chem. 288* (1956) 241.
11. Hahn, H. and Ness, P. *Naturwissenschaften 44* (1957) 534.
12. Hahn, H., Harder, B., Mutschke, U. and Ness, P. *Z. Anorg. Allg. Chem. 292* (1957) 82.
13. Hahn, H. and Ness, P. *Z. Anorg. Allg. Chem. 302* (1959) 37, 136.
14. Jellinek, F. *Ark. Kemi 20* (1963) 447.

Received January 27, 1975.